Central structure of low-n Balmer lines in dense plasmas*

John D. Hey†‡ and Hans R. Griem
Department of Physics and Astronomy, University of Maryland, College Park, Maryland 20742
(Received 15 July 1974; revised manuscript received 17 March 1975)

Stark-broadened profiles of the Balmer lines H_α and H_β have been measured by means of a high-pressure electromagnetically driven shock tube, at electron densities $N_e \sim 10^{17}$ cm^{-3} and temperatures $\kappa T \sim 1.5$ eV. The measured profiles of H_α, down to ~5% of peak intensity, are in much better agreement with the theoretical profiles of Kepple and Griem than with the results of more recent computations by Vidal, Cooper, and Smith. This suggests that for hydrogen lines with significant upper- and lower-state broadening, only *elastic* scattering contributions to the upper-lower state interference term should be included in the line-broadening operator. For H_β, agreement is obtained with both theories except within the central dip, the discrepancies between measured and predicted modulations being somewhat larger than those obtained in recent arc experiments. Our results for H_β can be interpreted as indicating the presence of a transition layer of much lower electron density near the walls rather than the necessity for including the effects of ion dynamics in the calculations. The first-order dynamical correction to the Holtsmark profile for a single Stark component is considered in analogy with stellar dynamics, and found to be of negligible importance under our conditions. Additional measurements of the central structure of D_β and the He I 4471-Å line are consistent with these conclusions.

I. INTRODUCTION

In this paper we consider two types of problems relating to the central structure in the Stark profiles of the lower members of the Balmer series: first, the disagreements between the computations of Kepple and Griem[1,2] and the results of calculations based upon the "unified theory" of Vidal, Cooper, and Smith[3,4]; second, disagreements between the results of both sets of calculations[1-4] and previous experiments,[5-10] as well as the investigation reported in this paper.[11,12] We are not concerned here with the relatively minor errors[10] resulting from the neglect of various sources of profile asymmetry, but with more substantial disagreements[11-13] which can be traced to considerations regarding some of the approximations[10] customarily made in Stark-broadening calculations, and which drastically affect the reliance which can be placed, for example, upon the width of the H_α profile in determining the electron density N_e.

Figures 1 and 2 represent some of the results of calculations by Kepple and Griem[1,2] (KG) and Vidal, Cooper, and Smith[3,4] (VCS) for H_α and H_β, for $N_e = 10^{17}$ cm^{-3} and $T = 20\,000$ °K. Normalized intensity $S(\alpha)$ is plotted against α, the wavelength separation in Å from line center divided by the Holtsmark normal field strength ($F_0 = 2.61 e N_e^{2/3}$). We note that a procedure of best-fitting experimental intensities to the H_α theoretical curve should result in about 90% higher electron density for the VCS calculation than one would obtain from KG, whereas in the case of H_β only a ~10% higher

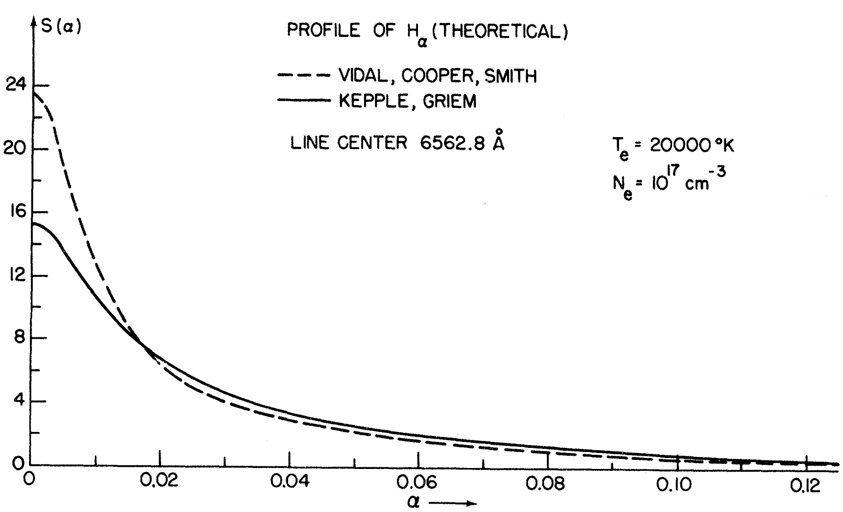

FIG. 1. Comparison of calculated H_α profiles.

electron density is predicted by VCS. An *inconsistency* therefore exists *within* at least one set of calculations.

A theoretical modulation for H_β may be defined as the difference between the maximum and central-minimum intensities, divided by the maximum intensity. Values of 37% and 41% are predicted by the KG[1,2] and VCS[3,4] theories, at $N_e = 10^{17}$ cm^{-3} and $T = 20\,000$ °K. Earlier arc experiments[6,8] had yielded modulations of only some 15% to 20%, depending upon the gas mixture in the arc, and the modes of observation and arc operation.

In attempting to account for the major differences between the calculated and observed central structure of H_β, as measured in this experiment[12] as well as in earlier work[5-10] and other experiments performed at the same time,[14] the following considerations have been suggested: first (from the theoretical point of view), the neglect of the effect of time-ordering of collisions in the evaluation of the line broadening operator $\mathcal{H}$ (see below), the neglect of dipole terms involving states of principal quantum number different from those of the initial and final states in the expression for $\mathcal{H}$ (i.e., neglect of "quenching" collisions and quadratic Stark effect), ion dynamical corrections to the static Holtsmark field, and thermal or suprathermal field fluctuations.[9,10] Second (from the "experimental" point of view), the question of plasma inhomogeneity (the effect of a transition layer near the walls or other density inhomogeneity) should be considered, at least in the case of the electromagnetic shock tube used in this experiment.

Of the various possible theoretical reasons advanced, the first may indeed be of some importance. However, judging from calculations[15] with and without time ordering for the H_α and L_β lines, it should fall well short of explaining the deviations quantitatively. For the second reason, the addition of such inelastic terms to the effective Hamiltonian leads again to a reduction but not elimination of the discrepancy within the dip of H_β,[16(a)] but substantially poorer agreement is in fact obtained over the profile as a whole.[10] For example, best-fit electron densities from line profiles are ~10% below electron densities measured interferometrically after inclusion of inelastic terms, while the two values agreed[16(b)] within ~3% before this modification. Moreover, the "strong collision term"[10] already includes some of these effects so that simply adding corrections for time ordering and inelastic collisions would clearly given an overestimate of their combined influence. It seems therefore rather safe to exclude these two mechanisms as major causes for the disagreement. We shall consider the questions of ion dynamical corrections, field fluctuations, and plasma inhomogeneity in some detail below.

II. EXPERIMENTAL METHOD AND RESULTS

For the purposes of an experimental investigation of the disagreements discussed above, a high-pressure electromagnetically driven shock tube[17,18] (length 86 cm, inner diameter 2.5 cm) was selected as the plasma source, and line profiles were scanned on a "shot-to-shot" basis.[11,12] Earlier investigations[19] showed that such devices[20] can produce rather homogeneous plasmas in a near thermodynamic equilibrium (LTE) state, and operate reproducibly.[17,18] A thin transition layer near the walls, of much lower electron density than the bulk plasma, had been detected interferometrically in an earlier experiment on a lower-pressure shock tube, but its presence was considered unimportant for the purposes of emission spectroscopy.[19(c)] A later investigation[21] verified that the assumption of local thermal equilibrium

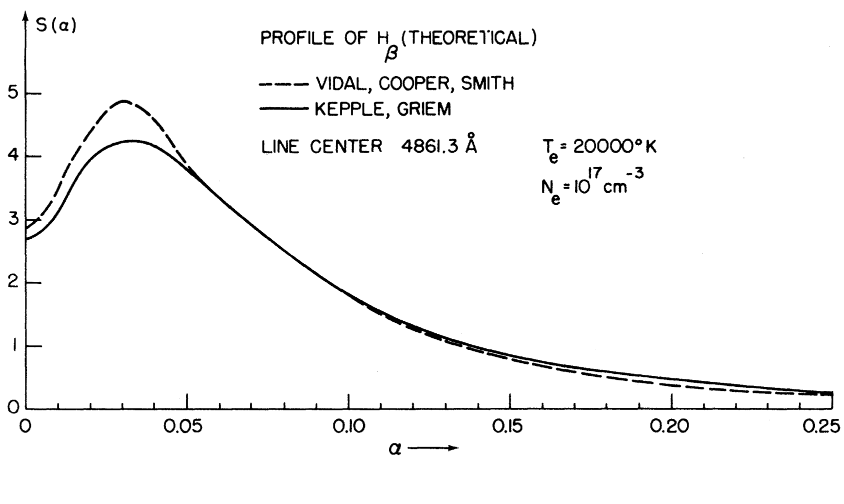

FIG. 2. Comparison of calculated H_β profiles.

for excitation and ionization of hydrogen atoms would be valid under our conditions. (The temperature, however, plays a very minor role compared with electron density, in the Stark broadening of spectral lines.) In the present experiment, helium was used as the carrier gas (ambient gas pressure ~20 Torr), with small (1% or less) admixture of molecular hydrogen in order to ensure that optical depth corrections remained small even near the center of H_α (since such corrections tend to suppress the major disagreement between the two theories). A plasma of electron density N_e ~10^{17} cm^{-3} and temperature $kT \sim 1.5$ eV was produced by discharging a bank of total capacitance 108 μF and firing voltage 8.5 kV, typical shock speeds being about 1 cm/μsec and the discharge period about 20 μsec. The useful lifetime of the plasma behind the reflected shock wave (the primary shock wave is not luminous) was 10–15 μsec for the profile measurements which were made by means of standard Jarrell-Ash half- and quarter-meter monochromators with auxiliary photomultiplier attachments. Corrections of tabulated profiles for Doppler and instrumental broadening were found to be of no practical significance, and it could readily be verified that other broadening mechanisms (van der Waals[22] and resonance broadening[23,24]) were completely negligible in the present experiment. Long-range collective effects[10,25–27] were ignored. Thermal field fluctuations are readily estimated not to change by much the instantaneous ionic field at the position of a given radiator, under the conditions of this experiment. Furthermore, there is no known mechanism to drive suprathermal field fluctuations (plasma instabilities) in this experiment. (In the case of nonhydrogenic systems one would expect the presence of plasma oscillations to be detectable as discrete resonances in a given line profile.[25])

Additional corrections of measured profiles for variations in window transmission throughout a given scan were kept small by observation of the plasma along a line of sight perpendicular to the axis of the shock tube, within approximately 1–3 mm of the reflector (an adjustable aluminum plate of diameter slightly less than that of the tube, which was used to define the total path length of the primary shock wave). A pair of pin-holes (500 μm in diameter), placed on the optic axis by a holder attached to the end of the tube (within which the reflector was now also housed, see Fig. 3), was separated by a distance equal to the inner diameter of the tube (2.5 cm) and besides defining the slab of plasma under observation, formed the outlet for the gas which was leaked into the tube through the discharge electrodes at a constant rate until a given firing of the bank, after which the inlet valve was closed and the tube evacuated (a rotary pump with liquid-nitrogen cold trap was adequate for the ambient pressures in this experiment). For further details on the circuitry associated with and operation of our electromagnetic shock tube, the reader is referred to Refs. 17, 28, and 29.

We now proceed to discuss diagnostic methods, the experimental results and their interpretation.

A. Diagnostic methods

The primary method of determining electron density involved a procedure to best-fit measured intensities at various wavelength points over the H_β profile, to theoretical tabulations of $S(\alpha)$ versus α (Sec. I above) with appropriate interpolation when necessary. Reproducibility of the plasma on a shot-to-shot basis was thus strongly relied upon; homogeneity (i.e., the possible effect of a tenuous cold layer near the walls or pin-holes) could be checked by omission of points near the center of the profile. The transition layer is discussed below; we point out here that on the whole a small change (a roughly 4–10% increase) in electron density was obtained from the computer program when points between the two H_β peaks were omitted. As will be seen from the tabulations[1,2,4] considered here (as well as the results of earlier calculations[30,31]) the method is temperature insensitive. The largest source of systematic error (of the order of 10%) was, however, found to be the actual choice of tabulated $S(\alpha)$ versus α. This is discussed in the section dealing with results, Sec. II G.

The best-fit program may be summarized as follows. For a set of m measured intensities

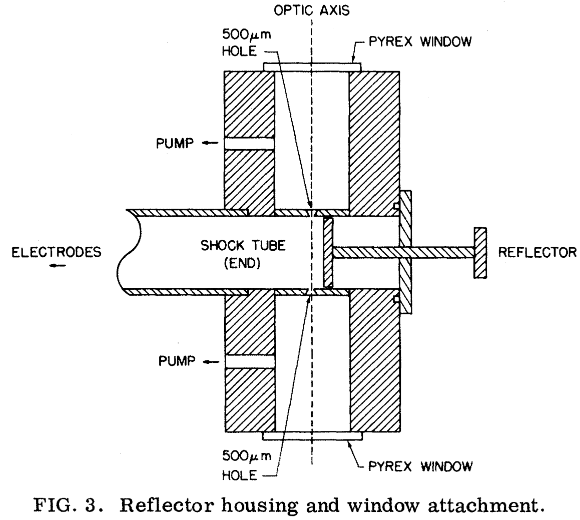

FIG. 3. Reflector housing and window attachment.

$I_i(\lambda_i)$, one considers the corresponding theoretical intensities (after converting to λ space) $(1/F_0) \times S_i(\alpha_i)$, where $\alpha_i = |\lambda_i - \lambda_0|/F_0$ and λ_0 is the wavelength at line center as measured by the particular monochromator, denotes the continuum intensity by C and the normalization factor by A, and forms the standard deviation squared:

$$\sigma^2 = \frac{1}{m-1} \sum_{i=1}^{m} \left(\frac{I_i - C}{A} - \frac{S_i}{F_0} \right)^2 . \tag{1}$$

For these purposes it is adequate to treat C as wavelength independent; "best" values of C and A may now be found from the conditions $\partial\sigma^2/\partial A = \partial\sigma^2/\partial C = 0$. For the computer program, the electron density is "guessed" (from a rough measurement of the linewidth) and this value is used at the start of a cycle of iterations on density which continues until successive values of σ^2 differ by sufficiently small amounts. This process is repeated for a series of λ_0 values in the vicinity of the apparent line center, until the minimum of σ^2 in the two-dimensional subspace (λ_0, N_e) has been found. The corresponding value of N_e is taken to be the best-fit electron density; percentage errors in the mean were found to be far smaller than the major systematic errors indicated above [choice of $S(\alpha)$, use or omission of points near line center]. In some cases (in connection with the measured H_α profile) it was found, owing to the large weights carried by the near-central points, that satisfactory continuum levels were not obtained by the above procedure, but that the *measured* continuum level should then rather be used as the value of C. The best-fit electron density was now determined subject to this constraint, with $\partial\sigma^2/\partial A = 0$.

In view of the importance of the full width of the H_β profile for diagnostic purposes in this experiment, it was of interest to make some assessment of the effect of the neutral-helium line λ4922 Å on the red wing of H_β. Detailed calculations of the profile of λ4922 Å for conditions at which the forbidden component (arising from mixing of the $4\,^1D$ and $4\,^1F$ levels by the plasma microfield) becomes important, have been performed by Barnard *et al.*[32] It was found that with omission of H_β points beyond about 4890 Å, the error in electron density from additional helium-line radiation should be below about 5%.

Additional estimates of the electron density were obtained from the full widths of neutral helium lines[10]; of these, the most suitable appeared to be He I λ6678 Å, in spite of the presence of a forbidden component in the vicinity of λ6630 Å on the blue wing which, according to recent measurements,[33] could result in about 10% reduction in width at $N_e \simeq 1.6 \times 10^{17}$ cm^{-3}. Some correction for optical depth at line center was also expected (~10%), and this was found to compensate to some extent for neglect of the forbidden component in width estimates. Owing to its narrow peak, this line is far more susceptible to the effects of shot-to-shot fluctuations than is H_β, and one would not expect an accuracy of greater than 10–15% in a value for N_e obtained in this way. Owing to the presence of the 500-μm pinholes on the optic axis, reliable values for electron density could only be obtained with great difficulty[29] from absolute continuum intensities[22] in the vicinity of λ5400 Å, and so this method was not generally adopted.

Values of C and A obtained by means of the minimizing procedure discussed in connection with the H_β profile [Eq. (1) above] provided a convenient way of obtaining the temperature (the line-to-continuum method[22,29]). The ~10% errors[22] incurred by the neglect of deviations from LTE of the helium level populations were of minor importance, and other approximations[29] for the total continuum emission from ionized helium were quite satisfactory for our purposes. (See Sec. II F for further non-LTE effects.)

Estimates of corrections owing to optical thickness, in the density and temperature ranges applicable to this experiment, show that radiative transfer is of some importance in the line core of H_α but a relatively minor effect for the higher series members. In comparing experimental results with theoretical profiles, the most convenient way to account for radiative transfer was first to apply optical depth corrections to the calculated values, and then compare these with measurements. The correction factor for optical depth to be applied to tabulated profiles is

$$(1 - e^{-\tau_\lambda})/\tau_\lambda ,$$

where $\tau_\lambda = k_\lambda l$ is the total optical depth of the (homogeneous) slab of plasma under observation (thickness l approximately equal to tube diameter), and k_λ is the effective absorption coefficient of the line.

Reproducibility of our plasma was monitored by selection of shots on the basis of fluctuations in total intensity of either a narrow neutral helium line (He I λ3889 Å) or the continuum in the vicinity of λ5400 Å, and also fluctuations in arrival time.

B. Measurement of the H_β profile

Since the profile of H_β was the primary means of obtaining electron densities for scans of H_α, we first discuss some detailed studies of its central structure. Table I presents a summary of the results obtained from scans in which a half-meter monochromator (except in the case of the first run) with instrumental width generally about 0.4 Å was used to scan the central region of the line profile, while a quarter-meter monochromator provided a detailed $[I(\lambda), \lambda]$ plot of the profile as a whole, from which values for the electron density and line-to-continuum ratio could be obtained. Distortions of the measured red wing of H_β owing to the He I λ4922-Å line could be eliminated satisfactorily by omission of points in the fit to theory.

Deviations between measured and theoretical points were, however, much more serious in the vicinity of line center, and a method of fitting was adopted whereby points were omitted from line center (also determined by the fit program) outward until good agreement, within a few percent, could be obtained with theory at the first included point. This generally occurred when the line peaks were reached; Figs. 4 and 5 show the excellent agreement obtained with, for example, the KG[1,2] calculations once the central points had been omitted. The change in apparent electron density is shown in the fourth column (Table I), where $\Delta N_e/N_e$ is the "final" value (with omission of cen-

TABLE I. H_β profile measurements.

Run No.	N_e (10^{17} cm^{-3})	Error (%)	$\frac{\Delta N_e}{N_e}$	T (°K)	Modulation (%)	Error (%)	Peak separation (Å)	P (%)
1	1.94	1	0.07	16 000	16.5 (12.5)	2	31	≃1
2(a)	1.94	1	0.01	18 500	17 (16.5)	2	28	≃1
2(b)	1.70	1	0.04	18 500	18 (17.5)	2	26	≃1
2(c)	1.51	2	0.10	17 500	18 (17)	2	21	≃1
3(a)	2.0	2	0.04	18 000	13.5 (12.5)	1	29	≃1
3(b)	1.73	2	0.04	17 000	15 (13.5)	2	25	≃1
3(c)	1.51	2	0.03	16 500	15.5 (14)	1	19	≃1
4(a)	1.04	2	0.07	17 500	14.5 (14)	2	19	1.04
4(b)	0.71	2	0.10	15 500	8 (7)	3	13	1.04
5(a)	0.97	1	0.13	17 000	12.5 (12)	2	16	1.04
5(b)	0.63	1	0.10	17 000	8 (7.5)	2	14	1.04
6(a)	1.40	1	0.09	17 000	12 (11)	1	22	1.04
6(b)	0.91	1	0.08	16 500	13 (12)	1	17	1.04

Additional electron-density values

Run No.	N_e (10^{17} cm^{-3})	Method
1	2.0	Width of He I λ3889 Å
4(a)	0.97	Absolute λ5400-Å continuum
4(b)	0.66	Absolute λ5400-Å continuum
6(a)	1.5	Width of He I λ6678 Å
6(b)	1.0	Width of He I λ6678 Å

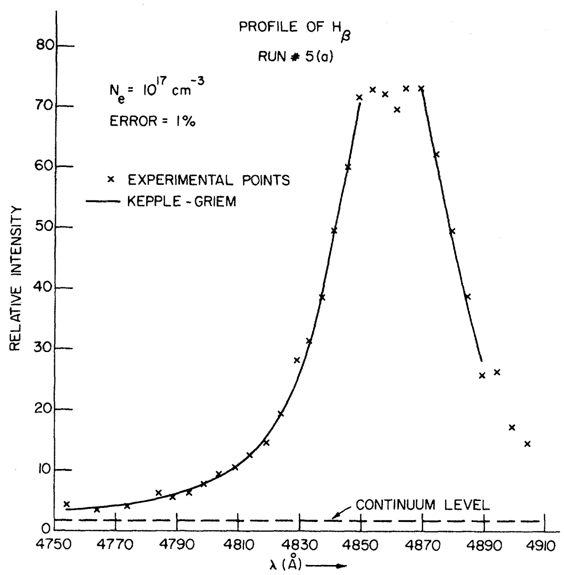

FIG. 4. Measured profile of H_β ($N_e = 1.0 \times 10^{17}$ cm^{-3}).

tral points) minus the "initial" value, divided by the final value of the electron density. The standard error in the mean for the final profile is given in the third column; the effective error in N_e from scatter of the points is thus about 1.5 times as great (from the error in the width), and this in turn is now clearly smaller than the error from *systematic* sources, one of the largest of which would be due to inclusion (or exclusion?) of the central points. The tabulated temperature (approximated to within 300 °K of the calculated value) is clearly susceptible to errors in the continuum level; these are estimated to result in an error below 1000 °K, probably about 500 °K. The reliability of the best-fit continuum level could readily be checked by comparison of the measured with "theoretical" points on the blue wing. The effect of an attempt to fit within the dip as well was most noticeable on the wings, where the theoretical curve then lies systematically above the experimental.

Another major source of systematic error in N_e would result, as was pointed out above, from the initial choice of theoretical profiles. For Table I we chose the KG[1,2] calculations. Fits to the VCS[4] computations are considered below; here we merely note that values of N_e obtained from the latter should be about 10% higher than those given in Table I. An error of $\sim\pm 4\%$ could typically be placed upon our tabulated N_e values provided that sources of systematic error have been properly dealt with. Additional electron-density estimates appear at the bottom of Table I, together with the method in each case. In spite of the larger uncertainties involved (see Sec. II A above) these values tend to confirm the above error estimate.

The percentage molecular hydrogen is given in the last column, with addition, for the last four runs, of the (here unimportant) percentage of background hydrogen as estimated for this device by Elton.[17]

Experimental values for the central modulation, as defined in the Introduction, are given in parentheses in the sixth column of Table I. They are obtained from a best fit to a quartic equation of the form

$$I(\lambda) - C = -a(\lambda - \lambda_0)^4 + b(\lambda - \lambda_0)^2 + c , \qquad (2)$$

of points lying in the vicinity of the central region, up to the peaks or slightly beyond, where the continuum (C) has been obtained from the fit to the "total" profile from which the electron density was determined. The (percent rather than fractional) modulation is thus

$$100 \frac{b^2}{4a} \left(c + \frac{b^2}{4a}\right)^{-1}$$

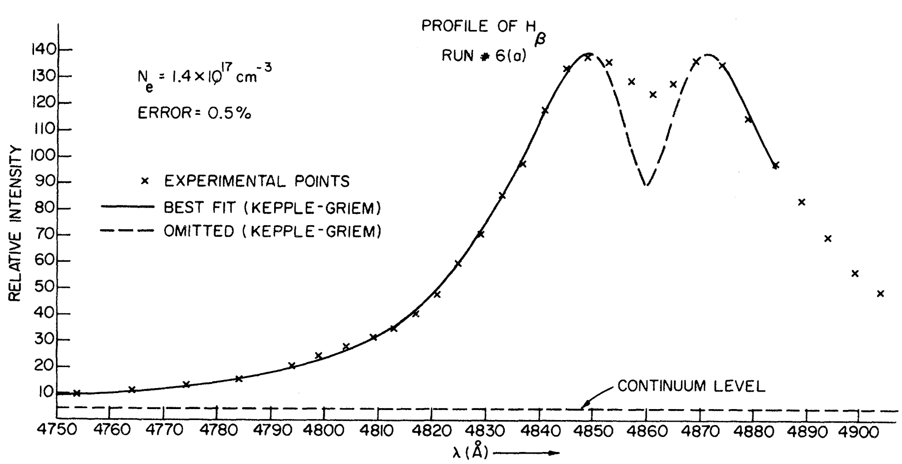

FIG. 5. Measured profile of H_β ($N_e = 1.4 \times 10^{17}$ cm^{-3}).

and the peak separation is given by $(2b/a)^{1/2}$.

The (absolute) errors in this modulation are found in the next column, and are estimated by twice the error in the mean of the fit to Eq. (2). Two factors clearly tend to reduce the modulation below the "true" value, first a finite instrumental width and second, radiative transfer. The first of these was unimportant except for the first run where subsequent correction resulted in a $\simeq 1.5\%$ increase. The second correction factor was computed from the measured temperature and density, with an effective plasma length equal to the inner diameter of the tube minus 1 mm at each wall. Resultant "corrected" modulations are listed above the measured value for each run. The total error in these is typically about ±3%, and they are seen to be fairly consistent with the results of earlier work,[5,6,8] apart from the rather low values obtained with lower electron densities [runs 4(b) and 5(b)], although the *interpretation* placed by some authors[14] upon the observed disagreement with theory requires careful consideration, as we show below.

C. Measurement of the He I 4471-Å profile

For greater insight into the problem of plasma homogeneity, it appeared to be of some interest to examine the profile of the He I λ4471-Å line, whose theoretical profile under our conditions is quite similar to that of H_β. In Table II, some results are listed of measurements of the dip between the allowed and forbidden components. For $N_e = 10^{17}$ cm^{-3} and $T = 20\,000$ °K, a value of 35% for the modulation is predicted by Griem[34] and Barnard *et al.*,[32] with a separation of 15 Å between the allowed $(4\,^3D \rightarrow 2\,^3P)$ and forbidden $(4\,^3F \rightarrow 2\,^3P)$ peaks; the width obtained from the more recent tabulations[32] is, however, smaller by about 8% than that found by Griem.[34] Note that "trivial" sources[10,22] of profile asymmetry, neglected in the calculations, would tend to reduce the apparent red-blue asymmetry. (More recent calculations by Deutsch *et al.*[35] are essentially in agreement, for our purposes, with the earlier work mentioned above, for electron density 3×10^{16} cm^{-3}.) To emphasize their similarity, we include a best fit of λ4471-Å points to the H_β theoretical profile for $N_e = 0.7\times10^{17}$ cm^{-3} (Fig. 6); an excellent fit is obtained, leading essentially to complete agreement in the predicted electron density from the two lines once an appropriate scaling factor has been introduced (from interpolations between given theoretical profiles[34]) for the dependence of width upon density. Note the appearance of the weaker $4\,^3P \rightarrow 2\,^3P$ forbidden component on the red wing.

The format of Table II follows exactly the description in connection with the H_β measurements; optical depth corrections were also estimated and found to be appreciable in one case only [2(a)]. For comparable densities, the modulations appear on the whole to be larger than in the case of H_β; however, the larger scatter in the points is clearly indicated by the seventh column. The relevant continuum level was harder to estimate in this case, owing particularly to the presence of the higher Balmer-series members of hydrogen, and errors in C could affect the tabulated modulation by an additional percent or more.

D. Measurement of the D_β profile

Experimental values of the modulation of the D_β line from a helium-deuterium plasma of comparable electron density and temperature to those already considered, are of interest in connection with the question of the importance of ion dynamical effects[12,14] on the central structure of the

TABLE II. He I 4471-Å measurements.

Run No.	N_e (10^{17} cm^{-3})	Error (%)	$\frac{\Delta N_e}{N_e}$	T (°K)	Modulation (%)	Error (%)	Peak separation (Å)	P (%)
1(a)	0.83	1	0.08	17 000	18	5	12	1.04
1(b)	0.51	2	0.11	17 500	17	4	10	1.04
2(a)	1.36	1	0.09	18 000	14.5 (14)	2	17	1.04
2(b)	0.91	1	0.07	16 500	15.5	3	14	1.04

Additional electron-density values

Run No.	N_e (10^{17} cm^{-3})	Method
2(a)	1.4	Width of He I λ6678 Å
2(b)	1.0	Width of He I λ6678 Å

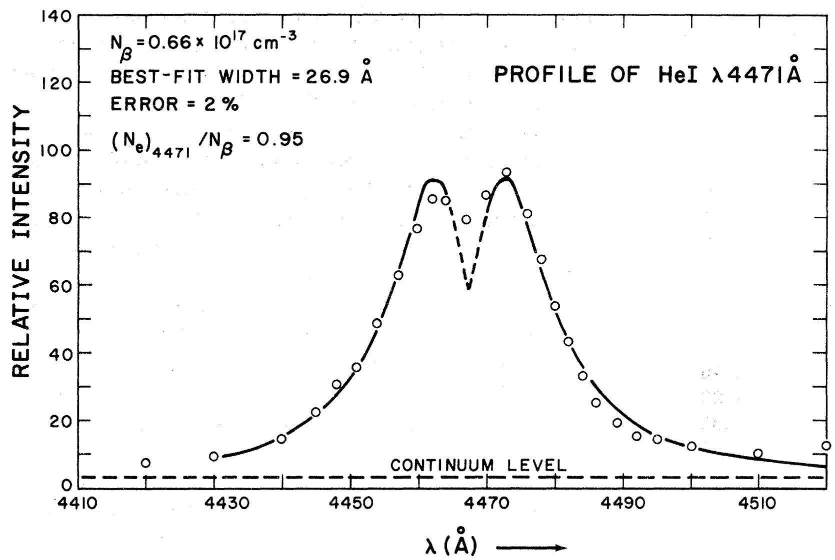

FIG. 6. Measured profile of He I λ4471 Å (N_e = 0.7 × 10^{17} cm^{-3}).

Balmer lines. Some results for such a plasma are listed in Table III; the notation is consistent with that explained in Sec. II B above. A complete profile of D_β is shown in Fig. 7, and may be compared with the very similar one for H_β (Fig. 5).

E. Discussion of profile discrepancies

We proceed now to the contention[14,35] that discrepancies between measured and calculated modulations for the lines discussed in Secs. II B–II D above, can be related to neglect of ion dynamical effects in the computations. It should, however, be stated that we have been unable to substantiate this contention on theoretical grounds[12,29] (see Sec. IV), at least as far as particle-produced fields are concerned.

When one attempts to find experimental evidence for a dependence of filling-in of the central dip upon reduced mass of the radiator-perturber combination, it is important to note the variation of predicted[1,4] modulation with electron density and temperature. In Table IV are listed values for the measured modulation, corrected for radiative transfer, and the relative modulation (the ratio of measured to interpolated theoretical modulation). Since we have various perturbing ions, we consider effective reduced masses μ_{eff}, where

$$\mu_{\text{eff}} = 0.5\left(\frac{N_{\text{H}^+}}{N_{\text{H}^+} + N_{\text{He}^+}}\right) + 0.8\left(\frac{N_{\text{He}^+}}{N_{\text{H}^+} + N_{\text{He}^+}}\right), \tag{3}$$

for example, in the case of H_β. N_{H^+} and N_{He^+} are

TABLE III. D_β profile measurements.

Run No.	N_e (10^{17} cm^{-3})	Error (%)	$\frac{\Delta N_e}{N_e}$	T (°K)	Modulation (%)	Error (%)	Peak separation (Å)	P (%)
1(a)	1.40	1	0.07	16 000	13.5 (11.5)	1	21	1.08
1(b)	0.90	1	0.06	17 000	13 (12.5)	1	17	1.08
2	0.90	1	0.11	16 500	12.5 (12)	1	18	1.08

Additional electron-density values

Run No.	N_e (10^{17} cm^{-3})	Method
1(a)	1.3	Width of He I λ6678 Å
1(b)	1.0	Width of He I λ6678 Å
2	0.9	Width of He I λ6678 Å

TABLE IV. Central modulations.

Run No.	N_e (10^{17} cm^{-3})	μ_{eff} ($m_{\text{H}}=1$)	Modulation (%)	Relative modulation
		(i) H_β		
1	1.94	0.54	16.5	0.52
2(a)	1.94	0.68	17	0.52
2(b)	1.70	0.69	18	0.55
2(c)	1.51	0.63	18	0.54
3(a)	2.0	0.65	13.5	0.42
3(b)	1.73	0.59	15	0.45
3(c)	1.51	0.63	15.5	0.46
4(a)	1.04	0.65	14.5	0.40
4(b)	0.71	0.55	8	0.22
5(a)	0.97	0.62	12.5	0.35
5(b)	0.63	0.65	8	0.21
6(a)	1.40	0.60	12	0.35
6(b)	0.91	0.59	13	0.37
		(ii) D_β		
1(a)	1.40	1.05	13.5	0.40
1(b)	0.90	1.14	12.5	0.35
2	0.90	1.10	12.5	0.35
		(iii) He I λ4471 Å		
1(a)	0.83	1.32	18	0.53
1(b)	0.51	1.58	17	0.44
2(a)	1.36	1.47	14.5	0.48
2(b)	0.91	1.16	15.5	0.46

the total particle densities of the hydrogen and helium ions, respectively. These densities are comparable, because hydrogen is almost fully ionized, helium only 1–2% for our conditions.

In comparing the results for H_β and D_β and noting the 1–5% experimental errors discussed in connection with Tables I–III, it is clear that on the whole, apart from two exceptional low-density runs, there is little evidence in these data for an increase in relative modulation with reduced mass. However, the higher accuracy of the three D_β runs compensates for their smaller number, and one can conclude that changing the reduced mass by ~2 gives at most a 4% change in the modulation. This upper limit is consistent with Ref. 14.

A systematic trend is observed when one attempts to classify the H_β data in groups of roughly the same electron density. Then, one finds that, in general, largest modulations are observed for the group with highest electron density and vice versa. Within the subclass $N_e \simeq 10^{17}$ cm^{-3}, modulations do in fact appear systematically lower than corresponding points for He I λ4471 Å, and noticeably so for $N_e < 8\times10^{16}$ cm^{-3}, say, by at least 3% in this case. This compares with an ~5% effect interpolated from the results of Ref. 14 for a factor ~3 change in the reduced mass.

It seems clear, however, that the spread within the H_β points cannot merely be discounted on the grounds of statistical fluctuations. For self-consistency, it now appears necessary to look for an explanation of these effects in terms of plasma homogeneity rather than ion dynamics. The trend noted above in connection with the H_β "points" would be an immediate consequence of the transition-layer "hypothesis" discussed below (since the shape of a narrower profile would be more readily affected by a given inhomogeneity).

When comparing our measured modulations with those given in Ref. 14, one finds that although the latter are systematically larger, they exhibit the same trend as we have already discussed, viz., for the *relative* modulation to increase with electron density.

F. Transition layer

We now proceed to what the present authors consider, at least in the case of the electromagnetic shock tube, to be the most plausible (experimental) explanation for the observed discrepancy between theory and experiment for the central structure of H_β.

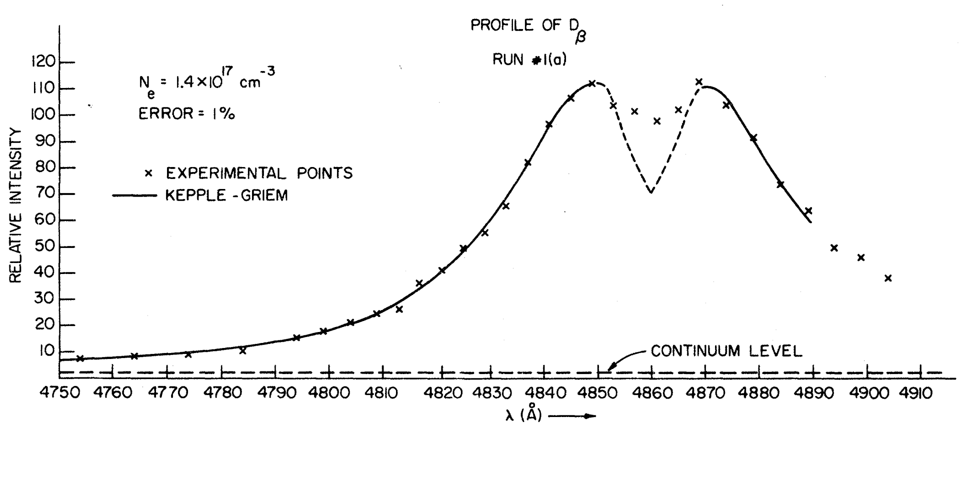

FIG. 7. Measured profile of D_β ($N_e = 1.4\times10^{17}$ cm^{-3}).

First, an attempt was made to construct an elementary two-layer model for the transition layer which could account for its main observable properties. Initially, two basic assumptions were made, viz., that the total pressure is uniform radially and that the percentage of atomic hydrogen ($2p$) is the same in the transition layer as in the main body of the plasma. Subject to these constraints, and with the further assumption that a semicoronal[22] model could be used to compute ion-to-neutral density ratios in the transition layer (with Saha decrements for hydrogen and helium, based upon the calculations of Drawin[36] and Drawin and Emard[37]), a relation[29] could be obtained for the electron density in the transition layer in terms of an *assumed* transition-layer temperature and given bulk parameters N_e and T. This equation could be solved by an iterative procedure alone, and yielded a plot of density versus temperature for the transition layer at the given bulk plasma conditions. The shape of the curve suggested a "model" whereby the average behavior is represented by a two-step function, i.e., that the transition layer might be treated as a single-layer homogeneous slab maintaining pressure balance with a hotter, more highly ionized homogeneous plasma. For example, for $N_e = 10^{17}$ cm^{-3} and $\kappa T = 1.55$ eV, one could deduce a transition-layer electron density of $\simeq 10^{16}$ cm^{-3} and temperature $\simeq 1$ eV.

The effect on such additional cool layers near the walls upon the H_β profile could be computed in the following manner. Assuming LTE for the upper level (energy E_u: even near the walls, the Saha decrement for hydrogen remains close to unity), one has for the intensity from some transition layer

$$I(\lambda) \propto \frac{N_e N_{H^+}}{F_0 T^{3/2}} S(\alpha) \exp\left(\frac{E_\infty - \Delta E_\infty - E_u}{\kappa T}\right)(2l') , \tag{4}$$

where E_∞ is the ionization energy for an isolated atom, reduced[22] by ΔE_∞ owing to plasma effects, and l' is the layer thickness. A similar relation holds for the bulk plasma, with the length $2l'$ replaced by $l - 2l'$, where l is the tube diameter. Figure 8 demonstrates that, with lengths l' of the order[19(a),19(c)] 1 mm ($l = 25$ mm, $l' = l'' = 1$ mm), an effective modulation of some 15% is readily obtained with a simple extension of this model to three layers, and that the corresponding change in measured electron density resulting from such a superposition of line profiles is in agreement with typical values for $\Delta N_e/N_e$ in Table I. [Note the smoothing out of the dip in the narrower profile produced by the outer transition layer, which becomes plausible when one considers enhanced gradient effects near the edge of this layer, as well as experimental resolution. The reason for the intermediate layer becomes apparent when one considers diffusion of helium ions (see below).]

The transition layer as described above would be too cool to radiate the neutral helium lines significantly. However, an important consideration, viz., gradient effects near the walls, has been ignored up to this point. Whereas the hydrogen-ion concentration, as computed above, would decrease by a factor rather less than an order of magnitude, the helium-ion concentration is calculated to decrease from $N_{He^+} \sim N_e$ to a negligible amount, $N_{He^+} \ll N_e$, from the bulk plasma to the walls. A diffusion of helium ions towards the walls would therefore be expected and their concentration thus would be above that calculated by the above procedure. The thickness of the transition layer may then be estimated by the mean free distance d for ionizing collisions, the calculation requiring merely the appropriate generalization[29] of results obtained earlier for a single species.[22] With approximate values for the relevant elastic and charge-exchange cross sections, one finds that $d \simeq 1$ mm. When one considers the total neutral

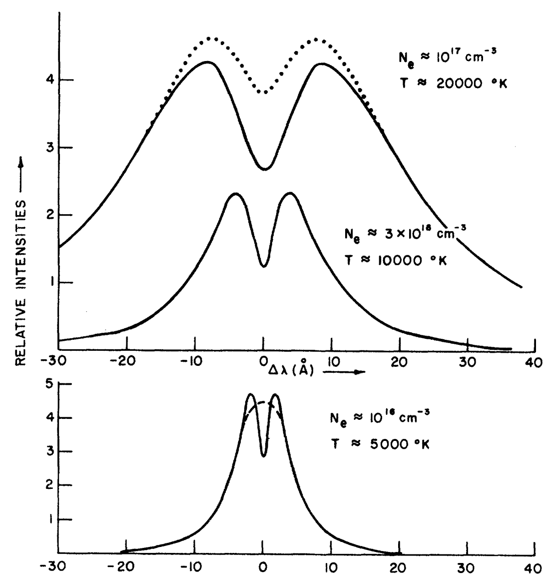

FIG. 8. Typical three-layer model for H_β modulation. The solid curves represent calculated line profiles for homogeneous layers of the indicated electron densities and temperatures, the dotted curve their weighted sum according to Eq. (4), except that the lowest density profile was smoothed as indicated by the dashed curve. Assumed lengths of the emitting layers are 21 mm for the bulk plasma and 1 mm each for the two transition layers on both sides of the bulk plasma. Hydrogen-ion densities are 3.8×10^{16} cm^{-3} in the bulk plasma and 1×10^{16} cm^{-3} in the transition layers, charge neutrality being provided by helium ions.

helium density near the walls, this diffusion represents a minor change in the total helium pressure, while providing a plausible mechanism to account for the filling-in of the He I λ4471-Å dip similar to that for H_β and D_β.

G. Measurement of the H_α profile

In Table V results are given for measurements of the profile of H_α from which the best-fit electron density N_α was obtained for the KG[1,2] and VCS[4] calculations; values of N_α were then compared with those (N_β) from the *corresponding* H_β profile for each case (according to the method outlined in Sec. II A, with instrumental corrections applied where necessary). Before fitting the measured H_α profiles to theory, tabulated values of $S(\alpha)$ were first corrected for the effects of radiative transfer (see Sec. II A above) with the electron density and temperature as obtained from the corresponding H_β profile. Approximate corrections at line center (for a homogeneous plasma) are given in the seventh column of the table.

For consistency, points in the immediate vicinity of the line center of H_α were also excluded from the H_α fits, as these would be most strongly influenced by the presence of plasma inhomogeneities. For numerical reasons, the magnitude of the effects of the latter on the H_α profiles is much harder to assess than in the case of H_β, where one has typically several points of comparable intensity within about 10 Å on either side of line center. However, by attempting to ensure that those near-central points on the H_α profile are omitted which correspond to the omitted points within the dip of the H_β profile, one is assured that possible effects of the transition layer are greatly diminished and one is then no longer concerned with the exact nature of the transition layer to the plasma under consideration (thickness ?, effect of pin-holes ?, etc.).

A suitable criterion for included points therefore appears to be:

$$\Delta\lambda = |\lambda - \lambda_0| \gtrsim \alpha_{\max} F_0[(\alpha_{1/2})_{H_\alpha}/(\alpha_{1/2})_{H_\beta}] \ , \qquad (5)$$

where[1] $\alpha_{\max}$ ($\simeq 0.033$ Å per cgs field strength at $N_e = 10^{17}$ cm^{-3}) corresponds to the peak of H_β and $\alpha_{1/2}$ is the half-width, in α space, of the respective lines. Thus (using KG[1,2] for $N_e = 10^{17}$ cm^{-3}), one should include only those points for which $\Delta\lambda \gtrsim 2$ Å under our conditions. Although this criterion was adhered to, excluded points (in the fit program) are plotted as well in Figs. 9 and 10 for H_α, and the corresponding theoretical curves extended up to line center from the regions

TABLE V. H_α profile measurements.

Run No.	N_β (10^{17} cm^{-3})	Error (%)	T (°K)	N_α (10^{17} cm^{-3})	Error (%)	Opacity[a] (%)	N_α/N_β	P (%)
				Kepple-Griem				
1(a)	1.62	2	18 000	1.44	1	22	0.89	0.23
1(b)	0.91	2	17 500	0.88	1	11	0.97	0.23
2(a)	0.91	1	17 500	0.97	1	11	1.07	0.23
2(b)	0.66	1	17 200	0.78	1	8	1.18	0.23
3	0.60	2	16 500	0.70	2	13	1.17	0.23
				Vidal, Cooper, Smith				
1(a)	1.77	2	18 200	2.96	1	34	1.67	0.23
1(b)	1.01	2	17 700	2.00	2	17	1.98	0.23
2(a)	1.03	1	17 700	2.04	1	18	1.98	0.23
2(b)	0.74	2	17 500	1.70	2	11	2.30	0.23
3	0.68	2	16 500	1.16	2	26	1.71	0.23

Additional electron-density values

Run No.	N_e (10^{17} cm^{-3})	Method
2(a)	0.86	Width of He I λ4471 Å
2(b)	0.68	Width of He I λ4471 Å

[a] Percent correction for optical depth.

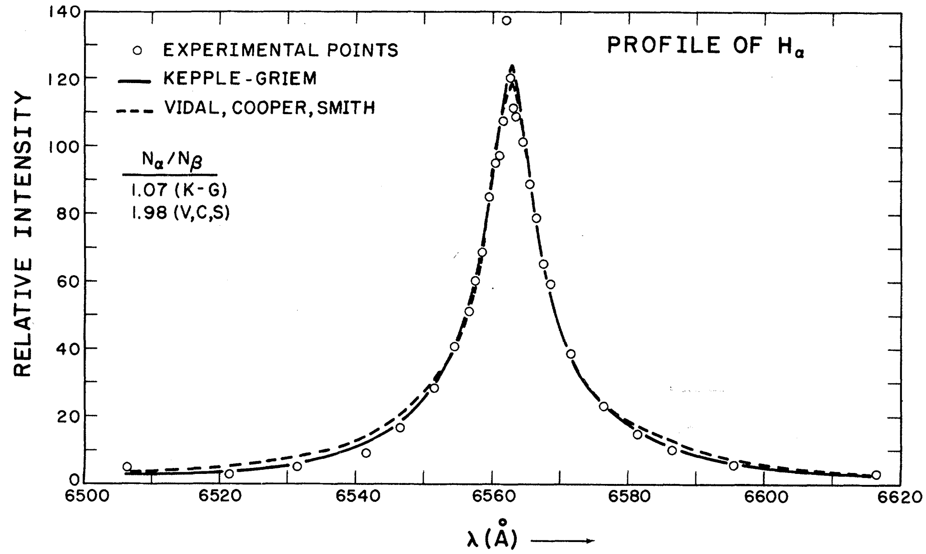

FIG. 9. Measured profile of H_α ($N_e = 0.9 \times 10^{17}$ cm^{-3}).

in which the fit was performed.

The major observation in Table V is the clear demonstration of inconsistency[11] of the electron densities obtained from the VCS[4] calculations for H_α with those from their H_β profiles for $N_e = 10^{17}$ cm^{-3}. By comparison, the KG[1,2] values for N_α and N_β are satisfactorily consistent. Apart from possible theoretical arguments (see Sec. III below), deviations of N_α/N_β of this order from unity could be attributed to statistical fluctuations (always of greater importance for H_α), remaining effects of the transition layer, and errors in opacity estimates and in instrumental corrections. These deviations are, however, clearly minor in comparison with the inconsistency in the VCS[4] calculations.

Support for these conclusions regarding the width of H_α is found in the work of Wiese *et al.*[8] and earlier experiments summarized in Refs. 2 and 8, while our observations are in strong disagreement with the recent arc experiment of Behringer[38] (where one notes that few measured points lie within the critical range about line center in which theoretical disagreements are the most significant). Behringer[38] reports "much better" agreement with the unified-theory calculations (VCS[4]) than with KG.[1,2] Ehrich and Kusch,[39] on the other hand, have recently published results of measurements of the widths of H_α and H_β from which electron densities N_α and N_β were obtained (using the KG[1,2] computations). Their values for N_α are consistently greater than those for N_β, the ratio N_α/N_β increasing with decreasing density, up to a factor of 5 for $N_\beta = 10^{16}$ cm^{-3}. Disagreement between N_α and N_β, using the VCS computations, should thus be as large as an order of magnitude, for $N_\beta = 10^{16}$ cm^{-3}, provided one were to assume that their experimental values for N_β are

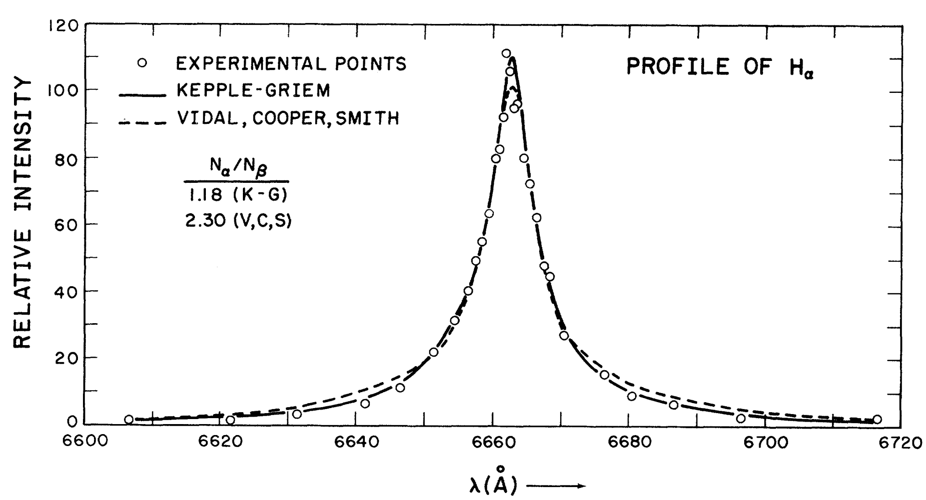

FIG. 10. Measured profile of H_α ($N_e = 0.7 \times 10^{17}$ cm^{-3}).

correct. Referring, however, to an earlier paper by Kusch,[40] one finds a similar disagreement between densities determined from the widths of He I $\lambda 5016$ Å or He I $\lambda 3889$ Å, and values for N_β, the latter being smaller by a factor of 1.7 in this case.

Our additional measurements of the widths of several neutral helium lines (Tables I–III, and V) lead to no such disagreement, supporting earlier results.[5,41] One is thus led to suspect that possible experimental reasons can be found for these discrepancies,[39,40] such as plasma inhomogeneities, instrumental broadening, or errors in optical depth corrections (where necessary).

III. SURVEY OF COMPUTATIONAL PROCEDURE

Equation (6) is the standard expression[1,2,10,22,30,31,42,43] for the shape of a Stark-broadened spectral line, where the notation of Baranger[44] has been employed, viz., that the set of initial (upper) states $\{|i\rangle\} \equiv \{|a\rangle, |b\rangle, |c\rangle \cdots\}$ which contribute to the line be denoted by Latin letters, whereas Greek letters indicate final (lower) states, $\{|f\rangle\} \equiv \{|\alpha\rangle, |\beta\rangle, |\gamma\rangle \cdots\}$:

$$L(\omega)=\frac{1}{\pi Z(T)}\int_0^\infty dF\,W(F)\,\mathrm{Re}\sum_{a,b,\alpha,\beta} e^{-E_a/\kappa T}\langle a|\vec{d}|\alpha\rangle\cdot\langle\beta|\vec{d}|b\rangle\left\langle\langle b\beta^*|\left[i\left(\omega-\frac{H_{Ai}(F)-H_{Af}^*(F)-\mathcal{H}}{\hbar}\right)\right]^{-1}|a\alpha^*\rangle\right\rangle . \tag{6}$$

If a diagonal representation is used for the atomic Hamiltonian H_A, the complex conjugate operation on H_{Af} may be omitted. Here $Z(T)$ is the atomic partition function, $W(F)$ the ionic field-strength distribution function and $\vec{d}$ the atomic dipole moment. The line-broadening operator $\mathcal{H}$ (*non-Hermitian*) is approximated[2] by

$$\mathcal{H}=-i\hbar\frac{4\pi}{3}\left(\frac{2m}{\pi\kappa T}\right)^{1/2}\left(\frac{\hbar}{m}\right)^2 N_e\langle v^{-1}\rangle^{-1} \times\left\langle v^{-1}(\vec{r}_i\cdot\vec{r}_i-2\vec{r}_i\cdot\vec{r}_f^*+\vec{r}_f^*\cdot\vec{r}_f^*) \times\left(\frac{1}{5}+\ln\frac{\rho_{\max}}{\rho_{\min}}+\frac{4}{3}\frac{\kappa T}{E_{\mathrm{H}}}\right)\right\rangle , \tag{7}$$

where $a_0\vec{r}$ is the position vector of the atomic electron; $\rho_{\max}$ and $\rho_{\min}$ are maximum and minimum impact parameters for broadening by electron collisions. The electron-velocity (v) distribution is usually taken to be Maxwellian. In the unified theory[3,4] (VCS), $\mathcal{H}$ becomes $\mathcal{H}(\Delta\omega)$, where $\Delta\omega=0$ at line center.

It will be found that outstanding theoretical disagreements relating to hydrogen-line-profile calculations can be traced to the manner in which some of the various approximations implied by Eqs. (6) and (7) are applied.[2,10,45] In particular, controversy still exists as to whether (a) it is adequate (incorrect?) to treat elastic and inelastic electron collisions on an equal footing in the evaluation[13] of $\mathcal{H}$, and (b) whether or not dynamical corrections should be applied to the static ion field.[12,14,46-48]

For the conditions of our experiment, we contend that inelastic electron collisions causing transitions between Stark-split sublevels of the same principal quantum number, are not in general consistent with the requirement of energy conservation except on the line wings ($\Delta\omega > \omega_p$).[13] Such terms should thus be omitted from the "interference" term in $\mathcal{H}$. The difficulty of the interference term is closely related to the neglect of perturber-perturber interactions in the impact approximation,[10] and some suggestions[13] can be made for an improved theory which employs quantized van Kampen[49] modes for the background plasma. Also in this connection it should be noted that because of the existence of an energy gap in the plasma spectrum corresponding to frequencies intermediate to ion and electron plasma frequencies, some objections[50] to the arguments in Ref. 13 are not conclusive. (A detailed discussion of these effects with numerical calculations will be the subject of a separate publication.[51]) Furthermore, we attempt to show that ion dynamical corrections are of negligibly small magnitude[12] in comparison with the discrepancies[5,6,8,14,29] between several experiments and both computations[2,4] for the central structure of H_β.

IV. ION DYNAMICAL CORRECTIONS

Lastly, we consider the importance of corrections for ion motion in a high-density plasma ($N_e \sim 10^{17}$ cm^{-3}). When one treats for simplicity the Holtsmark profile of a single Stark component, it can be shown[10,29,46] by analogy to stellar dynamics,[52] that the first-order dynamical correction is given by

$$l(\beta)-H(\beta)=\left(\frac{\omega_F}{\omega_S}\right)^2\left[\left(1+\frac{m_p}{m_r}\right)\Delta(\beta)+\frac{m_p}{m_r}\Delta'(\beta)\right] \tag{8}$$

subject to the condition that Debye shielding may be neglected (the masses m_p and m_r refer to those of a single perturber and radiator, respectively). Here β is the reduced ion field-strength F/F_0, with

$$F_0 = 2\pi(\tfrac{4}{15})^{2/3} |Z_p e| N_p^{2/3} , \tag{9a}$$

$$H(\beta) = \frac{2}{\pi\beta} \int_0^\infty x \exp[-(x/\beta)^{3/2}] \sin x \, dx , \tag{9b}$$

$$\Delta(\beta) = \frac{15}{64} \frac{d^3}{d\beta^3} \{\beta^{-1/2}[G(\beta) - I(\beta)]\} , \tag{9c}$$

$$\Delta'(\beta) = \frac{25}{256\pi} \frac{d^3}{d\beta^3} \left(\beta^{-2} \int_0^\beta H(\beta')\, d\beta' + \tfrac{13}{3}\beta^{-1} H - 2\frac{dH}{d\beta} \right) , \tag{9d}$$

$$I(\beta) = \frac{2}{\pi} \int_0^\infty x^{-5/2} \exp[-(x/\beta)^{3/2}] (\sin x - x \cos x)\, dx , \tag{9e}$$

$$G(\beta) = \beta \frac{dI}{d\beta} + \tfrac{3}{2} I(\beta) . \tag{9f}$$

The square of the ratio of characteristic frequencies for field fluctuations and Stark splitting is[46]

$$\left(\frac{\omega_F}{\omega_S}\right)^2 = \frac{4}{9(2.603)} \frac{\kappa T}{E_{\rm H}} \frac{m_e}{m_p} \times \left(a_0 N_p^{1/3} \frac{Z_p}{Z_r + 1} [n(n_1 - n_2) - n'(n_1' - n_2')] \right)^{-2} , \tag{10}$$

Z_p and Z_r being perturber and radiator charges, and the various n-s principal and parabolic quantum numbers.

The above treatment of the dynamical correction has several attractive features. First, it accounts for many-body interactions with the radiator, a *requirement* for small field strengths, i.e., near line center. (This is in contrast to several other treatments[47,48] of the dynamical correction.) The many-body nature of the problem in fact implies, *a priori*, that one cannot expect the dynamical correction to be inversely proportional to the reduced mass of a radiator-perturber pair, as some authors try to show.[14]

Second, the correction preserves the normalization of the line profile. From the limiting behavior of $H(\beta)$, $G(\beta)$, and $I(\beta)$ for small and large β, one can verify that

$$\int_0^\infty \Delta(\beta)\, d\beta = \int_0^\infty \Delta'(\beta)\, d\beta = 0 . \tag{11}$$

Third, it reduces to the Holstein result[53] for pair collisions on the far wings.

Two approximations of physical significance[10] were, however, made in this treatment. It was assumed that rotation of the axis of quantization (the instantaneous field direction), as well as off-diagonal matrix elements of the perturbing Hamiltonian, could be ignored. The results of the present theory can therefore only be expected to hold provided that the magnitude of the correction term is small compared to the Holtsmark function $H(\beta)$; this condition is found to be satisfactorily fulfilled over most of the line profile except in the immediate vicinity of line center ($\beta = 0$), where $\Delta(\beta)/H(\beta)$ and $\Delta'(\beta)/H(\beta)$ become very large. For example, in the case of a hydrogen atom perturbed by hydrogen ions, with $N_e = 10^{17}$ cm^{-3} and $\kappa T = 1.55$ eV, substitution into Eq. (8) leads to

$$l(\beta) = H(\beta) \left[1 + 0.0713 \left(\frac{2\Delta(\beta)}{H(\beta)} + \frac{\Delta'(\beta)}{H(\beta)} \right) \right] , \tag{12}$$

and using appropriate numerical values for $H(\beta)$, $\Delta(\beta)$, and $\Delta'(\beta)$, one finds that the correction term is negative for $\beta \lesssim 1$ and that $l(\beta)$ remains close to $H(\beta)$ for $\beta \gtrsim 0.25$, where $H(\beta)$ is already less than 10% of its peak value. Only within the range $\beta = 0$ to $\beta = 0.2$ is the magnitude of the correction comparable to or greater than that of $H(\beta)$.

Effectively, therefore, the region where the present theory is invalid corresponds to points well within the central dip of $H(\beta)$, where broadening by electron collisions dominates the actual line shape.

For the plasma conditions $N_e = 10^{17}$ cm^{-3} and $\kappa T = 1.55$ eV, the percentage correction to the Holtsmark profile referred to the peak is plotted in Fig. 11 for four radiator-perturber combinations: H-H$^+$, H-He$^+$, He-H$^+$, and D-D$^+$. This correction is seen to be extremely small, and could clearly not provide an explanation for the large discrepancy between the measured and calculated central dip of H$_\beta$. We note that dynamical corrections are largest outside the central dip and would probably first be observed as a steepening of the H$_\beta$ shoulders. Furthermore, the corrections are in fact *negative* near the line center (while positive on the wings), thus tending to enhance rather than reduce the dip.[12,29] While this conclusion differs from other predictions,[47,48] the typical magnitude of our correction is of the same order as those derived in rather different manners for H$_\beta$ by Lee[47] and for He I λ4471 Å by Segre and Voslamber.[54]

An estimate of the importance of Debye shielding is of some interest in the present context, and may be obtained through use of a screened Coulomb potential [screening length $\rho_D = (\kappa T/4\pi N_e e^2)^{1/2}$]. As discussed in Refs. 10, 29, and 46, the correction terms $\Delta(\beta)$ and $\Delta'(\beta)$ in Eq. (8) are directly related to fluctuation moments involving first time derivatives of the reduced field strength β [viz., $(\beta_x^{(1)})^2$, $(\beta_y^{(1)})^2$, etc.], where $\Delta(\beta)$ is the correction which one would obtain on the assumption of a stationary radiator, whereas $\Delta'(\beta)$ arises when one accounts for the additional effects of radiator motion against the background of perturbing particles. Upon evaluation of the fluctuation moments to order ρ_D^{-2}, one finds for example that at line center ($\beta = 0$) the contribution to $(\beta_x^{(1)})^2$ from the "stationary-radiator" term now increases by about 50% above the previous "unshielded" value, whereas the contribution from the "radiator-motion" term increases by a factor of about 2. While the correction to the Holtsmark profile is seen to remain unimportant under our conditions, we note that in this case Debye shielding tends to enhance the importance of the radiator-motion term or, in other words, further reduces the *direct* dependence upon the reduced mass of the radiator-perturber pair (i.e., the many-body nature of the problem is enhanced, as one would expect).

A more complete calculation of the effects of Debye shielding is perhaps of interest for possible application of the present theory to astrophysical and laboratory plasmas of lower density, where dynamical corrections to the quasistatic broadening by ions would be more important.

V. CONCLUSIONS

Our conclusions regarding the central structure of H_α and H_β refer basically to questions regarding: (i) the inclusion (or exclusion?) of inelastic electron scattering contributions to the upper-lower state interference term in the expression for the electron broadening operator; (ii) the importance of ion dynamics in accounting for discrepancies between theory and experiment, particularly in the case of H_β; (iii) other possible mechanisms such as plasma inhomogeneities which might account for these differences.

In connection with (i) above, our measurements of the H_α profile indicate that although plasma inhomogeneities could account to some extent for the disagreement between theory and experiment, the presence of a transition layer to our shock-tube plasma plays a *minor* role in comparison with the very large disagreement between the two theories.[1-4] An inconsistency in the more recent computations[4] for H_α and H_β is clearly demonstrated. This seems to suggest also on experimental grounds that the exclusion of inelastic electron scattering contributions to the interference term in $\mathcal{H}$ is warranted.

We believe that a more complete theory, accounting for interactions between the perturbing electrons and the background plasma would be expected to diminish drastically such inelastic terms for frequency separations from line center less than the plasma frequency (i.e., except on the far wings). Other effects, like time-ordering and collision-induced transitions to states of different principal quantum number should be numerically less important. For example, a recent calculation[55] gives an increase in the half-width by a factor ~1.2, rather than a factor ~1.6 as found experimentally.

Referring next to (ii) above, we must state that our measurements of the central modulation of H_β could not confirm, but are within experimental errors consistent with a simple relationship[14] be-

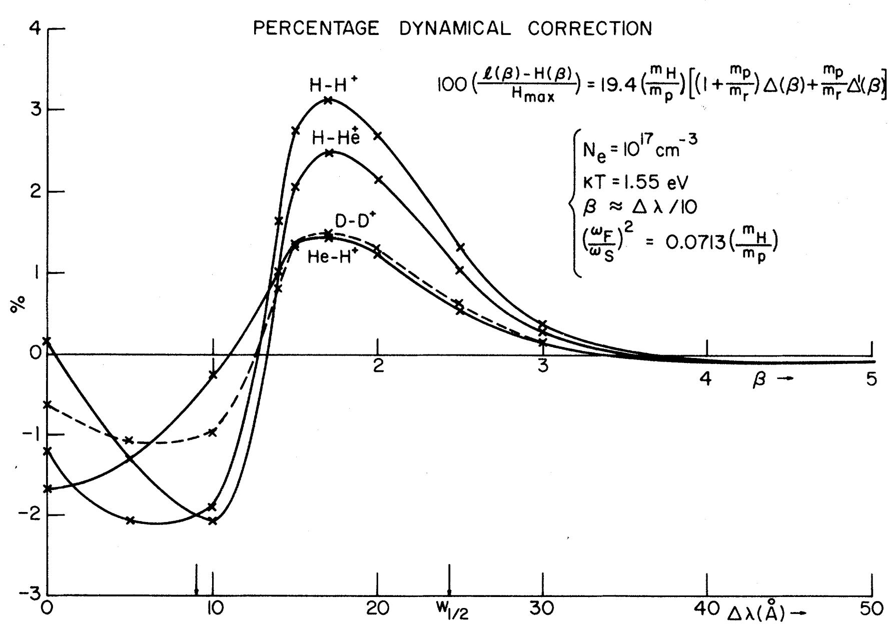

FIG. 11. Percentage dynamical correction for a typical Stark component (arrows indicate approximate positions of H_β peak and half-intensity points).

tween deviations from theory and the reduced mass of the perturber-radiator combination. Our measured profiles seem to be influenced by a thin transition layer to our plasma which, while affecting the H_β linewidth to a minor extent only, could account quite plausibly for the discrepancy between measured and calculated[1,2,4] modulations [point (iii) above]. Computations[10,29,56] of ion dynamical corrections to the Holtsmark profile of a single Stark component indicate that the quasistatic approximation for ions remains a very good one under our conditions even in the immediate vicinity of line center. While these calculations do not include Debye shielding, our estimates of the fluctuation moment $(\beta_x^{(1)})^2$ to second order in ρ_D^{-1} show that allowance for screening effects will not alter our basic conclusion.

Although our estimates indicate that the effect of thermal field fluctuations is small in our plasma in comparison with individual ion contributions to the effective field strength at the position of the radiator, we suggest that a laser scattering experiment could be undertaken to determine the level of such fluctuations. A study by Kato[57] indicates that even in a plasma with as few as two electrons in a Debye sphere, the usual light scattering theory (derived for the condition $\frac{4}{3}\pi\rho_D^3 N_e \gg 1$) obtains, and thus the fluctuation spectrum in laser light scattered from such a shock-tube plasma could perhaps also be determined in a similar manner. Any nonthermal density fluctuations (arising from plasma instabilities), which we have already discounted in our case, would be detected in such an experiment.

---

*Work supported by the National Aeronautics and Space Agency and the National Science Foundation.

†Present address: Physics Department, University of Cape Town, Rondebosch 7700, Cape, South Africa.

‡Some of the material in this paper is part of a Ph.D. thesis (University of Maryland, 1974); see Ref. 29.

[1]P. Kepple, University of Maryland Technical Report No. 831, 1968 (unpublished).
[2]P. Kepple and H. R. Griem, Phys. Rev. 173, 317 (1968).
[3]E. W. Smith, J. Cooper, and C. R. Vidal, Phys. Rev. 185, 140 (1969).
[4]C. R. Vidal, J. Cooper, and E. W. Smith, Astrophys. J. Suppl. 25, 37 (1973).
[5]H. F. Berg, A. W. Ali, R. Lincke, and H. R. Griem, Phys. Rev. 125, 199 (1962).
[6]C. H. Popenoe and J. B. Shumaker, Jr., J. Res. Natl. Bur. Stand (U.S.) A 69, 495 (1965).
[7]H. R. Griem, Comments At. Mol. Phys. 2, 103 (1970).
[8]W. L. Wiese, D. E. Kelleher, and D. R. Paquette, Phys. Rev. A 6, 1132 (1972).
[9]H. R. Griem, Comments At. Mol. Phys. 3, 181 (1972).
[10]H. R. Griem, *Spectral Line Broadening by Plasmas* (Academic, New York, 1974).
[11]J. D. Hey and H. R. Griem, Bull. Am. Phys. Soc. 18, 660 (1973).
[12]J. D. Hey, Bull. Am. Phys. Soc. 18, 1343 (1973).
[13]H. R. Griem, Comments At. Mol. Phys. 4, 75 (1973).
[14]D. E. Kelleher and W. L. Wiese, Phys. Rev. Lett. 31, 1431 (1973).
[15]M. E. Bacon, Phys. Rev. A 3, 825 (1971); J. Quant. Spectrosc. Radiat. Transfer 12, 519 (1972).
[16](a) R. A. Hill and P. Kepple, Sandia Laboratories Report SC-M-70-584, 1970 (unpublished); (b) R. A. Hill, J. B. Gerardo, and P. C. Kepple, Phys. Rev. A 3, 855 (1971).
[17]R. C. Elton, U.S. Naval Research Laboratory Report No. 5967, 1963 (unpublished).
[18]R. C. Elton and H. R. Griem, Phys. Rev. 135, A1550 (1964).
[19](a) E. A. McLean, C. E. Faneuff, A. C. Kolb, and H. R. Griem, Phys. Fluids 3, 843 (1960); (b) W. L. Wiese, H. F. Berg, and H. R. Griem, Phys. Rev. 120, 1079 (1960); (c) E. A. McLean and S. A. Ramsden, Phys. Rev. 140, A1122 (1965).
[20]A. C. Kolb, Phys. Rev. 107, 345 (1957).
[21]T. N. Lie, M. J. Rhee, and E. A. McLean, Phys. Fluids 13, 2492 (1970).
[22]H. R. Griem, *Plasma Spectroscopy* (McGraw-Hill, New York, 1964).
[23]A. W. Ali and H. R. Griem, Phys. Rev. 140, A1044 (1965).
[24]A. W. Ali and H. R. Griem, Phys. Rev. 144, 366 (1966).
[25]M. Baranger and B. Mozer, Phys. Rev. 123, 25 (1961).
[26]H.-J. Kunze and H. R. Griem, Phys. Rev. Lett. 21, 1048 (1968).
[27]H. R. Griem and H.-J. Kunze, Phys. Rev. Lett. 23, 1279 (1969).
[28]J. D. E. Fortna, U.S. Naval Research Laboratory Report No. 6950, 1969 (unpublished).
[29]J. D. Hey, University of Maryland Technical Report No. 74-089, 1974 (unpublished).
[30]H. R. Griem, A. C. Kolb, and K. Y. Shen, U.S. Naval Research Laboratory Report No. 5805, 1962 (unpublished).
[31]H. R. Griem, A. C. Kolb, and K. Y. Shen, Astrophys. J. 135, 272 (1962).
[32]A. J. Barnard, J. Cooper, and L. J. Shamey, Astron. Astrophys. 1, 28 (1969).
[33]J. R. Greig, L. A. Jones, and R. W. Lee, Phys. Rev. A 9, 44 (1974).
[34]H. R. Griem, Astrophys. J. 154, 1111 (1968).
[35]C. Deutsch, M. Sassi, and G. Coulaud, Ann. Phys. (N.Y.) 83, 1 (1974).
[36]H. W. Drawin, *Reactions under Plasma Conditions*, edited by M. Venugopalan (Wiley-Interscience, New York, 1971), Chap. 3.
[37]H. W. Drawin and F. Emard, Z. Phys. 243, 326 (1971).
[38]K. Behringer, Z. Phys. 246, 333 (1971).
[39]H. Ehrich and H. J. Kusch, Z. Naturforsch. A 28, 1974 (1973).
[40]H. J. Kusch, Z. Naturforsch. A 26, 1970 (1971).
[41]J. R. Greig and L. A. Jones, Phys. Rev. A 1, 1261 (1970).

[42]M. Baranger, Phys. Rev. 112, 855 (1958); A. C. Kolb and H. Griem, Phys. Rev. 111, 514 (1958).
[43]H. R. Griem, A. C. Kolb, and K. Y. Shen, Phys. Rev. 116, 4 (1959).
[44]M. Baranger, Phys. Rev. 111, 494 (1958).
[45]H. R. Griem, Phys. Rev. 140, A1140 (1965).
[46]H. R. Griem, Comments At. Mol. Phys. 2, 19 (1970).
[47]R. W. Lee, J. Phys. B 6, 1060 (1973).
[48]J. Cooper, E. W. Smith, and C. R. Vidal, J. Phys. B 7, L101 (1974).
[49]N. G. Van Kampen, Physica 21, 949 (1955).
[50]D. Voslamber, Bull. Am. Phys. Soc. (to be published).
[51]H. R. Griem, P. C. Kepple, and J. J. Perez-Esandi (unpublished).
[52]S. Chandrasekhar and J. Von Neumann, Astrophys. J. 95, 489 (1942); 97, 1 (1943).
[53]T. Holstein, Phys. Rev. 79, 744 (1950).
[54]E. R. A. Segre and D. Voslamber, Phys. Lett. 46A, 397 (1974).
[55]L. J. Roszman, Phys. Rev. Lett. 34, 785 (1975).
[56]H. R. Griem and J. D. Hey, Bull. Am. Phys. Soc. 19, 585 (1974).
[57]M. Kato, Phys. Fluids 15, 460 (1972).